

Temporal stability analysis identifies soil water relations under different land use types in an oasis agroforestry ecosystem



Yongkun Zhang^{a,d}, Qingli Xiao^c, Mingbin Huang^{a,b,*}

^a State Key Laboratory of Soil Erosion and Dryland Farming on the Loess Plateau, Institute of Soil and Water Conservation, CAS&MWR, Yangling 712100, China

^b Institute of Soil and Water Conservation, Northwest A&F University, Yangling 712100, China

^c College of Resources and Environment, Northwest A&F University, Yangling 712100, China

^d University of Chinese Academy of Sciences, Beijing 100049, China

ARTICLE INFO

Article history:

Received 29 August 2015

Received in revised form 14 February 2016

Accepted 21 February 2016

Available online 3 March 2016

Keywords:

Soil water variation
Land use pattern
Groundwater recharge
Root water uptake

ABSTRACT

The spring wheat–shelterbelt–maize agroforestry ecosystem is one of the most common land use patterns occurring in oasis agriculture in the arid zones of northwest China. Soil water interactions were hypothesized to exist between adjacent land use types, and that these interactions could be analyzed by using the soil water content (SWC) measured at the most time-stable locations (MTSLs) under each land use type. Objectives of this study were to (1) identify the MTSLs for the different soil layers under each land use type and (2) to investigate the soil water relations between adjacent land use types using the SWC measured at the identified MTSLs. The SWC was measured in 2012 and 2013 at 10-cm depth intervals within 0–260 cm soil profiles at 36 locations along three transects that passed through spring wheat, shelterbelt, and maize subplots. A time-stability analysis of SWC was used to identify the MTSLs in the four different soil layers under each of the three land use types. The results indicated that temporal variations in soil water in the same soil layer among the three land use types tended to have similar patterns. The SWC of the different soil layers under maize exhibited the highest temporal stability among the three land use types. The SWC measured at the MTSLs identified for each soil layer under each land use type was proven to represent their mean SWC. Correlation analyses of the SWCs measured at the MTSLs between two land use types indicated that soil water relations occurred between adjacent land use types but not between those that were non-adjacent land use types by the correlation analyses of the SWCs measured at the MTSLs between two land use types. In the upper soil layer (0–200 cm), soil water relations were mainly affected by shelterbelt root water uptake from the adjacent cropland into which the tree roots had extended. In the lower soil layer (200–260 cm), the soil water relations among the three land use types were due to groundwater recharge, which was a result of crop irrigation that had raised the water table to a level at which it could replenish this soil layer.

© 2016 Elsevier B.V. All rights reserved.

1. Introduction

Sandy desertification is an important environmental problem confronting oasis-agricultural ecosystems (Luo et al., 2005). In order to protect the cropland against damage from sandstorms and dry thermal winds originating in deserts, shelterbelts have been planted around and within the oasis areas. However, perennial trees have greater water consumption than annual crops (Ong et al., 1992; Williams et al., 2009). In order to develop sustainable management systems of limited water resources, it is essential to know about the soil water variations and relations that occur within and among the different land use types that comprise an agroforestry ecosystem.

The Heihe River is one of the largest inland rivers in the arid zones of northwest China. The Heihe River Basin (HRB) supports oasis agriculture that is of great significance to the social and economic development of the region. One of the most common land use patterns used in the oasis agriculture is spring wheat–shelterbelt–maize agroforestry. Past studies of soil water under oasis agricultural systems have mainly focused on the relations between soil water and plant species diversity (Li et al., 2008), and on the spatial variability of soil water within the oasis-desert (Wang et al., 2007) and cropland–shelterbelt–desert ecotones (Shen et al., 2014). However, few studies have considered the spring wheat–shelterbelt–maize land use pattern as an entire continuum when investigating soil water variations and relations within it. Such knowledge would be of importance to the management of the limited basin water resources.

An agroforestry ecosystem refers to land use systems in which woody perennials are purposely planted in the same land management units as agricultural crops (Nair, 1985; Nestel, 1983). In such a system,

* Corresponding author at: State Key Laboratory of Soil Erosion and Dryland Farming on the Loess Plateau, Institute of Soil and Water Conservation, Northwest A&F University, Yangling 712100, China.

E-mail address: hmingbin@yahoo.com (M. Huang).

the effects on soil water variations are more complex under the combination of trees and seasonal crops than under the same trees and crops when grown separately. Soil water variations within an agroforestry ecosystem depend on many factors, including the tree and crop species, the proportions of land area allocated to the crops and the trees, root distributions, soil properties, and the prevalent climate. Another factor is the proximity of the crops to the trees and/or the pattern of their distributions in relation to each other. Previous studies had shown that trees could extract water from the soil in adjacent cropland areas, and that this depended on the type of agroforestry system (Ellis et al., 2005; Knight et al., 2002; Malik and Sharma, 1990). The SWCs under crops were depleted to a greater extent by tree root water uptake as the distance from the trees became shorter (Huxley et al., 1994; Livesley et al., 2004; Shen et al., 2014; Woodall and Ward, 2002). Similar results were obtained for adjacent land use types by Ellis et al. (2005) who studied cropland and shelterbelt systems and by Knight et al. (2002) who investigated shelterbelt and pasture interactions.

Understanding the temporal variability of soil water is essential to water resources management. The concept of time stability, which was first proposed by Vachaud et al. (1985), is useful when investigating SWC variability over time. It enables the time-invariant relations between SWC (or another soil property) at a given spatial location and its basic statistical parameters to be characterized. Kachanoski and Jong (1988) developed the concept of time stability of soil water at specific sampling locations to encompass the temporal persistence of spatial soil-water distribution patterns, which was determined by using Spearman rank correlation analysis between successive time intervals. One of the most useful practical applications of the time stability concept is to find the most time-stable locations (MTSLs) that can then represent the mean SWC for a given area (Brocca et al., 2009; Grayson and Western, 1998; Hu et al., 2009, 2010; Martínez-Fernández and Ceballos, 2005; Liu and Shao, 2014).

Agroforestry systems are commonplace in all ecological and geographical regions of world (Nair, 1993). Therefore, understanding of soil water relations among the different land use types of such agroforestry systems is important in order to increase the water use efficiency

of the whole system as well as the crop productivity. We hypothesized that soil water interactions existed between adjacent land use types, and that these interactions could be analyzed by using the SWC measured at the MTSLs under each land use type. The main objectives were to: (1) identify the MTSLs for the different soil layers under the three land use types comprising the agroforestry ecosystem and (2) to investigate the soil water relations between adjacent land use types using the SWC measured at the identified MTSLs.

2. Materials and methods

2.1. Study area

The study area is at the Linze Ecological Observational and Experimental Station (39°21'N, 100°07'E), which is located in a desert-oasis ecotone in the middle reach of the HRB of Northwest China (Fig. 1). The site is characterized by continental arid temperate climate conditions, with a mean annual precipitation of 116.8 mm (1965–2000), about 90% of which falls during the rainy season between June and September. The mean annual air temperature is about 7.6 °C, and varies between the mean minimum temperature of −27.8 °C in December and the mean maximum temperature of 39.1 °C in August. The mean annual open water evaporation is about 2365 mm (Chang et al., 2006). The mean frost-free period is 165 days, and the relative humidity ranges from 7.3% to 80.9% (Chang et al., 2006). The area is densely vegetated with crops (mainly maize, *Zea mays* and spring wheat, *Triticum spp.*) and shelterbelts consisting mostly of Gansu Poplar (*Populus gansuensis*).

2.2. Experimental design and measurements

An 80 m × 16 m experimental plot was established that included three subplots along its length. In sequence, these were a spring wheat subplot, a shelterbelt subplot, and a maize subplot with length of 22, 36, and 22 m, respectively (Fig. 2). Thus, the shelterbelt was bordered to the south by spring wheat and to the north by maize. The shelterbelt had nine rows of Gansu Poplars, which were planted in 1980

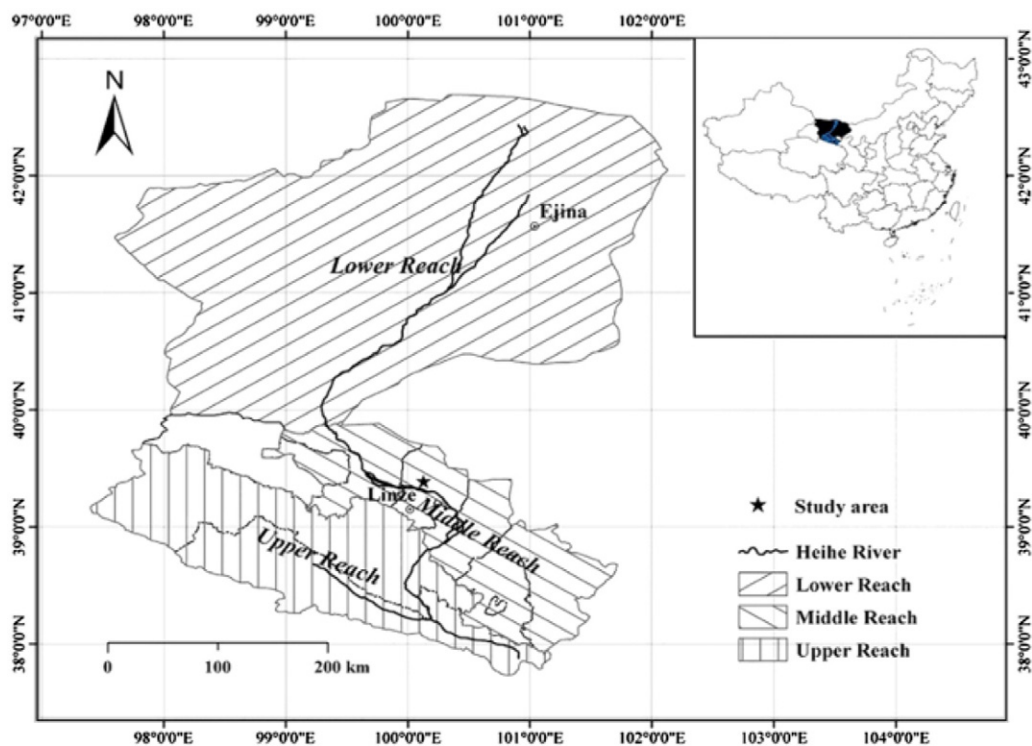


Fig. 1. Location of the study area in the Heihe River basin, China.

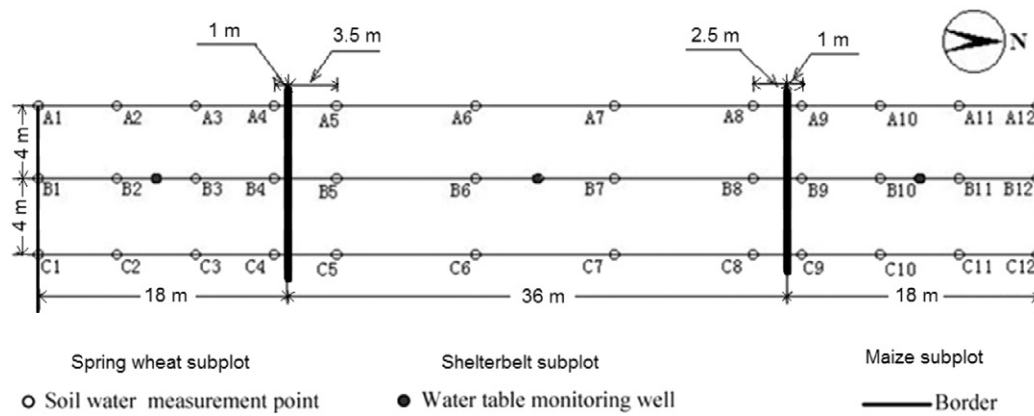


Fig. 2. The layout of the experimental plot.

with a row spacing ranging from 4.45 to 6.7 m. The growing season of the Gansu Poplars was from May to October, whereas those of the spring wheat and maize were from March to July and April to September, respectively.

During the growing seasons, the cropland was irrigated by conventional flood irrigation once every 7 to 14 days with an irrigation amount of approximately 100 mm per irrigation event. A similar irrigation amount was applied at the beginning of the winter season after sowing both crops. The amount of irrigation was intended not only to meet the crop water requirements but also to leach the soil profile of salts in order to avoid problems related to increased salinity. As shown in Fig. 3, 21 irrigation events occurred in the spring wheat subplot during the studied period (nine events in 2012 and 12 events in 2013), while 24 irrigation events occurred in the maize subplot (12 events in both 2012 and 2013). Daily rainfall and other climatic variables were recorded by an AG1000 automated weather station at a distance of about 500 m from the study site. During the experimental period, there were 21 rainfall events in 2012 and 25 rainfall events in 2013, which produced total rainfall amounts of 84.4 and 73.2 mm, respectively. For the 46 rainfall events, the mean rainfall depth, storm duration, rainfall intensity, and interval time between two successive rainfall events were 4.3 mm, 4.3 h, 0.84 mm/h, and 287.4 h, respectively.

Three parallel transects were laid out along the length of the spring wheat-shelterbelt-maize plot, with a spacing of 4 m (Fig. 2). Twelve Trime-Time Domain Reflectometry (TDR) access tubes (4-cm diameter, polycarbonate) were installed to a depth of approximately 280 cm in each subplot (Fig. 2). Four access tubes were located along each of the three transects passing through a given subplot in order to facilitate the measurement of volumetric SWC. The distance between adjacent

tubes along a transect in the wheat and maize subplots was 5.67 m, while in the shelterbelt subplot it was 10 m. The three land use types were considered as different treatments, while the 12 locations in each land use type (3 transects \times 4 locations along each transect) were treated as replications. Since the 12 locations were not randomly distributed within each land use type, this experimental design involved pseudo-replication (Hurlbert, 1984).

Volumetric SWC was determined by a calibrated Trime-TDR probe (TRIME-TDR-PICO-IPH-T3, Imko, Germany) at 10-cm depth intervals to a depth of 260 cm, around which depth the level of the water table frequently fluctuated. Measurements were made every 3–5 days, and additional measurements were made before and after irrigation events, and after rainfall. Monitoring of SWC was carried out from April 25 to September 12 in 2012 and from April 25 to September 22 in 2013. The Trime-TDR was calibrated in the field under both dry and wet conditions against the calculated volumetric SWC of collected samples. Two locations in each land use type were selected to collect the calibrated soil samples at every 10-cm depth increment from the surface to the depth of 280 cm using a coring device during the period of TDR tube installations, for which SWC was first determined using the gravimetric method. A calibration curve was obtained between the TDR-derived SWC (TDR, $\text{cm}^3 \text{cm}^{-3}$) and the gravimetrically-derived volumetric SWC (θ , $\text{cm}^3 \text{cm}^{-3}$) as follows:

$$\text{SWC} = 0.871\text{TDR} + 0.041 \quad R^2 = 0.86. \quad (1)$$

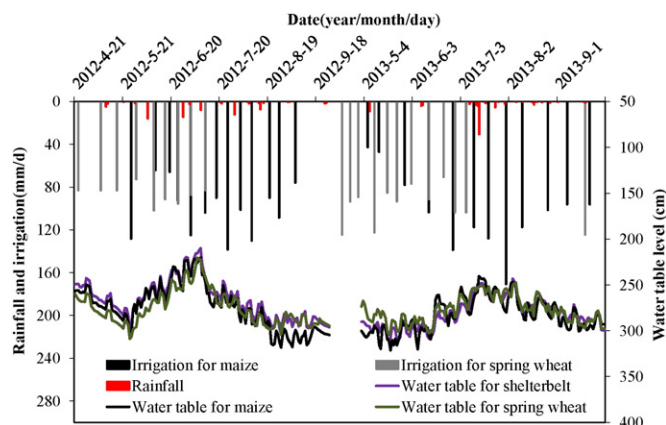


Fig. 3. Rainfall and irrigation events and variations in the water table level during the observation periods of 2012 and 2013.

The soil particle-size distributions of collected soil samples were determined by laser diffraction (Laser Scattering Particle Size Distribution Analyzer Model LA-950, Horiba Instruments Inc., 2008). The disturbed soil samples used for soil particle size determination were collected at 10-cm depth intervals down to a depth of 100 cm, and at 20-cm intervals between the depths of 100 and 260 cm at each TDR tube location during augering prior to the insertion of the TDR tubes into the soil. In addition, a soil profile pit, 260 cm deep, was dug in each land use subplot for each transect. Undisturbed soil samples were taken from the soil profile at every 20-cm depth increment using standard pre-weighed 100-ml Kopecki rings. These soil samples were used to determine bulk density by the gravimetric method (ASTM C29/C29M-09, 2003). The mean bulk density profile was calculated using the three replications, which were taken from the corresponding soil depths of each of the three profile pits in a given land use subplot. The soil profile was divided into four layers (0–30 cm, 30–120 cm, 120–200 cm, and 200–260 cm) based on the distributions of the measured soil properties (Table 1). The mean SWC for the individual 0–30, 30–120, 120–200, and 200–260 cm layers as well as for the entire soil profile (0–260 cm) at a given measurement time were calculated by weighting the soil water content against the corresponding soil layer thickness.

Table 1
Soil physical properties in the spring wheat, shelterbelt, and maize subplots.

Land use type	Soil layer (cm)	Soil texture			Bulk density (g cm ⁻³)	Soil type
		Clay (%)	Silt (%)	Sand (%)		
Spring wheat	0–30	14.06 ± 2.64 [#]	19.78 ± 3.60	66.16 ± 3.04	1.43 ± 0.03	Sandy loam
	30–120	13.46 ± 1.1	13.42 ± 1.96	73.11 ± 3.59	1.55 ± 0.03	Sandy loam
	120–200	16.23 ± 2.10	15.23 ± 1.91	68.54 ± 2.51	1.52 ± 0.01	Sandy clay loam
	200–260	8.68 ± 1.89	10.69 ± 1.11	80.63 ± 3.65	1.54 ± 0.02	Sandy loam
Shelterbelt	0–30	20.82 ± 2.55	30.32 ± 2.34	48.87 ± 2.83	1.39 ± 0.02	Clay loam
	30–120	18.24 ± 1.07	18.89 ± 1.72	62.87 ± 2.56	1.60 ± 0.02	Sandy clay loam
	120–200	35.86 ± 2.16	36.71 ± 1.99	27.43 ± 1.28	1.49 ± 0.02	Loamy clay
	200–260	19.24 ± 1.06	22.91 ± 1.64	57.85 ± 1.12	1.53 ± 0.01	Sandy clay loam
Maize	0–30	24.02 ± 1.05	36.64 ± 2.27	39.35 ± 2.67	1.41 ± 0.02	Clay loam
	30–120	29.17 ± 1.61	28.14 ± 1.28	42.69 ± 2.72	1.57 ± 0.03	Loamy clay
	120–200	32.34 ± 1.49	35.44 ± 2.74	32.22 ± 1.18	1.51 ± 0.02	Loamy clay
	200–260	16.98 ± 1.94	29.13 ± 1.71	53.89 ± 2.46	1.54 ± 0.02	Clay loam

[#] Indicates the mean ± standard error.

One groundwater level monitoring well was established in each land use subplot along the middle transect (Fig. 2). The water table level was automatically recorded every 20 min by a water-level logger (Hobo U20-001-04, Onset Computer Corporation, Bourne, USA).

2.3. Assessment of temporal stability

The time stability of the SWC was investigated using the relative difference analysis (Vachaud et al., 1985). The temporal deviation at a given location was indicated by the standard deviation of the temporal mean relative difference. In order to derive this value, the mean of the relative difference, δ_{ijk} , of the SWC measured in a given soil layer, at a particular location and on a specific date, θ_{ijk} , was calculated by:

$$\delta_{ijk} = \frac{\theta_{ijk} - \bar{\theta}_{jk}}{\bar{\theta}_{jk}} \quad (2)$$

where for every land use type, i is the location ($i = 1, 2, 3, \dots, N$; $N = 12$), j is the soil layer ($j = 1, 2, 3, \text{ or } 4$; where $j = 1$ refers the uppermost soil layer, 0–30 cm), and k is the measurement time ($k = 1, 2, 3, \dots, M$; $M = 30$ in 2012, and $M = 37$ in 2013), and $\bar{\theta}_{jk}$ is the mean SWC at each time, k , in a particular layer j , which is given by:

$$\bar{\theta}_{jk} = \frac{1}{N} \sum_{i=1}^N \theta_{ijk} \quad (3)$$

Then, for a given location, i , the temporal mean relative difference, $\bar{\delta}_{ij}$ (MRD) and its standard deviation $\sigma(\delta_{ij})$ (SDRD), over time were calculated by:

$$\bar{\delta}_{ij} = \frac{1}{M} \sum_{k=1}^M \delta_{ijk} \quad (4)$$

$$\sigma(\delta_{ij}) = \sqrt{\frac{1}{M-1} \sum_{j=1}^M (\delta_{ijk} - \bar{\delta}_{ij})^2} \quad (5)$$

Generally, sampling locations that had relatively lower values of SDRD were regarded as the locations with higher time stability (Grayson and Western, 1998).

2.4. Selection of time-stable locations

Representative locations are usually defined as the locations where the SWC values are close to the field mean value (Vanderlinden et al., 2012). Zhao et al. (2010) proposed an index of time stability (ITS) combining the MRD and its SDRD to determine the time-stable locations as:

$$ITS_{ij} = \sqrt{\bar{\delta}_{ij}^2 + \sigma(\delta_{ij})^2} \quad (6)$$

The ITS provided a single metric that could identify the best sampling locations that would be representative of the mean field SWC (i.e., low $\bar{\delta}_{ij}$) and that were also temporally stable (i.e., low $\sigma(\delta_{ij})$). In this study, the time-stable locations were selected as those having ITS values lower than 5%, and the MTSLs were identified as those having the smallest ITS values within a subplot.

To analyze the temporal stability of the SWC, the dataset was divided into two groups. The measured dataset for 2012 was used as a calibration dataset that identified the MTSLs for each of the four soil layers under each land use type, while the measured dataset from 2013 was used as a validation dataset that tested the accuracy, for each land use type, of the measured SWC at the MTSLs when used to estimate the mean SWC.

2.5. Statistical analyses

Considering that the SWC measurement locations were not selected randomly and independently, a mixed-effects model with spatially correlated errors was used to investigate land use and soil layer effects on SWC and correlations of SWC between different land use types and between soil layers (Lark and Cullis, 2004; Beguería et al., 2013; Hu et al., 2015). The generalized least squares (GLS) model which splits the variable of interest (i.e., SWC) into the deterministic component, spatially correlated residue, and uncorrelated residual was applied. The residual maximum likelihood (REML) method was used to fit the GLS model in order to estimate the variance parameters because the study experimental design involved pseudo-replication and the REML method is unbiased (Lark and Cullis, 2004). The SAS software was used for all statistical analyses (SAS Institute Inc., 2008).

3. Results

3.1. Soil water variations under different land use types

3.1.1. Temporal variations of soil water

The time series of the mean SWC determined for a given soil layer on a specific date under each of the three land use types are presented in Fig. 4, while Table 2 presents the correlation coefficients for the SWC between any two different soil layers under a particular land use type. In the spring wheat subplot (Fig. 4a), the SWC in the 0–30 cm soil layer was similar to that in the 30–120 cm soil layer, while overall in the four layers they tended to increase with increasing soil depth. Significant correlations ($p < 0.01$) were mainly found between two soil layers that were adjacent (Table 2). In the deepest (200–260 cm) soil layer, the mean SWC was significantly greater ($p < 0.01$) than those in the upper three soil layers (0–30, 30–120, and 120–200 cm), which were not significantly different from each. In the maize subplot, significant correlations ($p < 0.01$) were found between any two soil layers within their

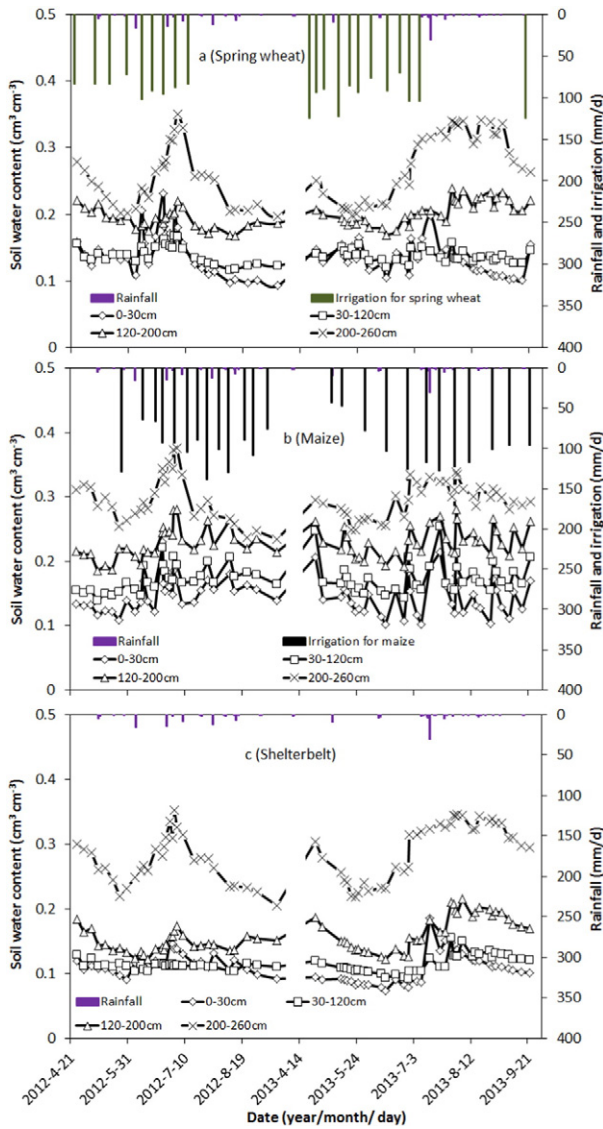


Fig. 4. Changes in soil water contents in the four soil layers under spring wheat, maize and shelterbelt subplots.

respective profiles, although correlations were stronger, as indicated by higher correlation coefficient values between two adjacent layers than between two non-adjacent layers. The mean SWC values were

Table 2
Correlation coefficient matrix for soil water contents in four soil layers under each of the three land use types.

	0–30 cm	30–120 cm	120–200 cm	200–260 cm
Spring wheat				
0–30 cm	1.00			
30–120 cm	0.86**	1.00		
120–200 cm	0.13	0.39**	1.00	
200–260 cm	0.23	0.32**	0.75**	1.00
Maize				
0–30 cm	1.00			
30–120 cm	0.89**	1.00		
120–200 cm	0.74**	0.85**	1.00	
200–260 cm	0.39**	0.43**	0.63**	1.00
Shelterbelt				
0–30 cm	1.00			
30–120 cm	0.51**	1.00		
120–200 cm	0.47**	0.87**	1.00	
200–260 cm	0.64**	0.58**	0.74**	1.00

** Significance level less than 0.01.

significantly different ($p < 0.01$) among all four soil layers and increased with increasing soil layer depth (Fig. 4b). Similarly, in the shelterbelt subplot (Fig. 4c), mean SWCs followed the same pattern of increase with soil depth. However, the mean SWCs were only slightly greater in the 30–120 cm soil layer than in the 0–30 cm layer during most of the observation period. Mean SWCs in the deepest soil layer were significantly greater ($p < 0.01$, $N = 67$) than those in the upper layers.

Variations in SWC in each soil layer presented similar trends for all land use types during 2012 and 2013 (Fig. 4). In 2012, SWCs tended to initially decrease throughout the profile before increasing from about June 5, reaching maximum values on slightly different dates just before July 10; they then tended to decrease while fluctuating. In 2013, SWCs tended to decrease throughout the whole profile before June 13th, although the minimum values were attained in the deepest layer by the end of May. After mid-June, SWCs tended to increase to different extents and to fluctuate due to irrigation and rainfall events.

3.1.2. Profile distribution of soil water

The profiles of the mean SWCs are shown in Fig. 5 for the three land use subplots. The soil water profiles could be divided into two layers under the spring wheat and shelterbelt. The uppermost of these soil layers (0–120 cm) was characterized by SWCs at different depths that were similar. Consequently, the SWC within this layer was almost constant but tended to increase with increasing depth. In the second layer (120–260 cm), the SWC increased more rapidly with depth, from 0.147 to 0.314 $\text{cm}^3 \text{cm}^{-3}$ under spring wheat and from 0.116 to 0.362 $\text{cm}^3 \text{cm}^{-3}$ under the shelterbelt. In contrast, under maize, the SWC tended to increase at a relatively steady rate. However, there was a notable decline in the SWC at depths between 200 and 210 cm. The mean SWCs in the 0–200 cm layer were significantly different ($p < 0.01$) among the three land use types. However, in the profile below a depth of 200 cm, there were no significant differences among the SWCs under the three land use types.

The variations in the soil water profiles on different dates for the three land use types are presented in Fig. 6. For both the spring wheat and shelterbelt subplots, the changes in the soil water profiles among different dates were similar (Fig. 6a and b). In the 60–170 cm layer, there was little change in the SWC over time. However, the SWCs below 170 cm were significantly different ($p < 0.01$) on different dates under both spring wheat and trees. In contrast, the soil water profile under maize exhibited greater changes over time that were due, at least in part, to responses to irrigation events (Fig. 6c).

3.2. Groundwater level variations under different land use types

Groundwater level fluctuated with the irrigation events and the water level of the Heihe River. At the commencement of the study period in 2012, the water level fell and reached the lowest value of 308 cm on May 25. Then, it began to rise and reached a peak value of 220 cm on July 5. Afterwards, the water level declined to 312 cm at the end of the first study period. During the next study period of 2013, the water level declined to the lowest value of 321 cm on May 18 and rose to the highest value of 250 cm on July 14; it then fluctuated around 250 cm (Fig. 3). The rise in the water table depth always lagged about 1 or 2 days behind irrigation occurrences. The mean groundwater level was 280 cm under spring wheat, 282 cm under maize, and 276 cm under the shelterbelt, no significant differences in groundwater level ($p < 0.01$) were found among them.

3.3. Temporal stability of soil water contents under different land use types

3.3.1. Temporal stability during the calibration period

The ranked MRD of the SWCs with the corresponding SDRD presented as error bars, along with the ITS values, are presented in Fig. 7 for the four soil layers at each sampling location under the three different land use types, while their statistical values are given in Table 3. The

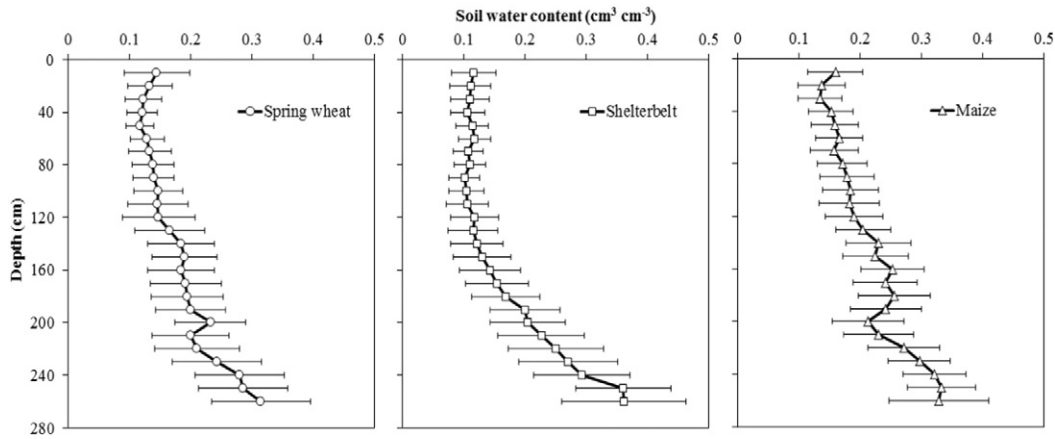


Fig. 5. The mean soil water content profile under spring wheat, shelterbelt, and maize during the study period. The error bars represent the standard error for the mean values.

temporal stability of the SWC values under maize was the greatest in each soil layer as compared with the layers under spring wheat and trees (Table 3). The spring wheat and shelterbelt subplots had similar SWC temporal stability in each soil layer. However, a comparison of means showed that there were no significant differences ($p < 0.01$) under the three land use types in the SWC temporal stability of the two deeper soil layers (120–200 cm; 200–260 cm). However, there were significant differences in the SWC temporal stability of the two upper soil layers (0–30 cm; 30–120 cm).

3.3.2. Estimation of mean soil water contents using measurements made at the MTSL

The MTSLs for each soil layer under the three land use types were determined by the lowest values of ITS, which are depicted by the empty symbols in Fig. 7. Hence, the respective MTSLs identified for the four soil layers under each land use type were: locations C₃₋₁, C₁₋₂, A₃₋₃ and A₄₋₄ in the spring wheat subplot; A₇₋₁, A₈₋₂, A₈₋₃ and C₅₋₄ in the shelterbelt subplot; and C₁₀₋₁, C₁₀₋₂, C₁₂₋₃ and A₁₁₋₄ in the maize subplot.

The measured SWC at the MTSLs during the validation period of 2013 were plotted against the calculated mean values as shown in Fig. 8 for the four soil layers under each of the three land use types. Linear regression showed that the measured SWCs at the MTSLs were significantly correlated ($p < 0.01$) with the calculated mean values and, therefore, that these measured SWC values at the MTSLs could be used to estimate the mean SWC values in all of their respective soil layers under their respective land use type. Among the three land use types, the values measured at the MTSLs in the maize subplot gave the most accurate estimation of the mean SWC in the four layers as

indicated by the higher r values. The least accurate estimations of the SWC were obtained for every layer under the shelterbelt.

Fig. 9a shows the MRD values of SWC, calculated using all SWC measurements in the 2-year experimental period, for four soil layers at 36 sampled locations. The ranges between the minimum and maximum values in the 0–30, 30–120 and 120–200 cm soil layers were relatively similar, and were greater than that of the 200–260 cm soil layer. The SWC values at the locations closed to the borders between cropland and shelterbelt were drier than the mean in croplands, hence exhibiting negative MRD values (i.e. A₃, B₃, C₃, B₄, C₄, A₈, B₈, C₈, A₉, B₉, C₉, A₁₀, B₁₀). The cumulated ITS values were also computed for all sampled locations (Fig. 9b). An inspection of Fig. 9b reveals that the 30–120 and 200–260 cm soil layers had similar and lower ITS values, as compared to the 0–30 and 120–200 cm soil layers. The maize subplot had a mean ITS value of 14.7% lower than that in spring wheat (19.2%) and shelterbelt (18.8%) subplots.

3.4. Soil water relations between adjacent land use types

The SWC measurements made at the MTSLs were used to analyze the soil water relations between adjacent land use types. The correlation coefficient was used to assess the similarity of the SWC temporal patterns among the different land use types (Table 4). Temporal patterns of the SWC distributions in the 200–260 cm soil layer were significantly correlated ($p < 0.01$) among all three land use types. In the 0–30 and 120–200 cm soil layers, significant correlation ($p < 0.01$) only occurred between adjacent subplots, while no significant correlations ($p < 0.01$) were found among the subplots for temporal SWC distributions in the 30–120 cm soil layer. Therefore, the SWC measured at the MSTLS

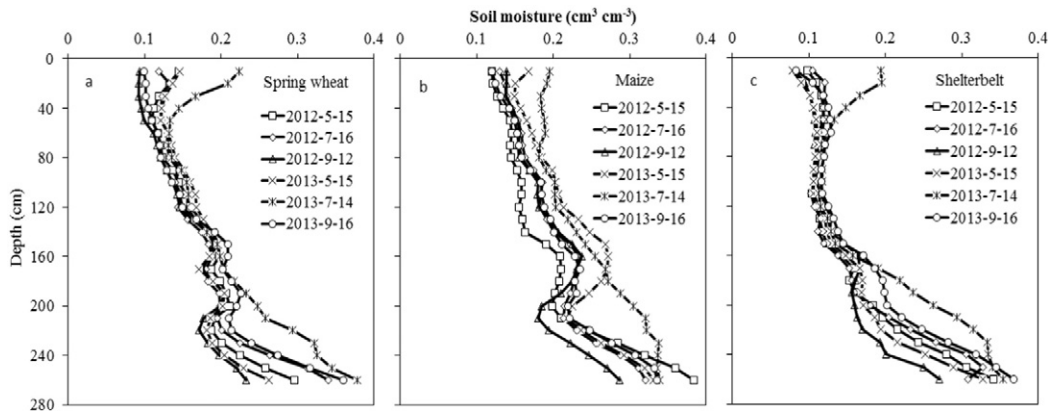


Fig. 6. Soil water content profiles under (a) spring wheat, (b) maize, (c) shelterbelt, and on specific dates.

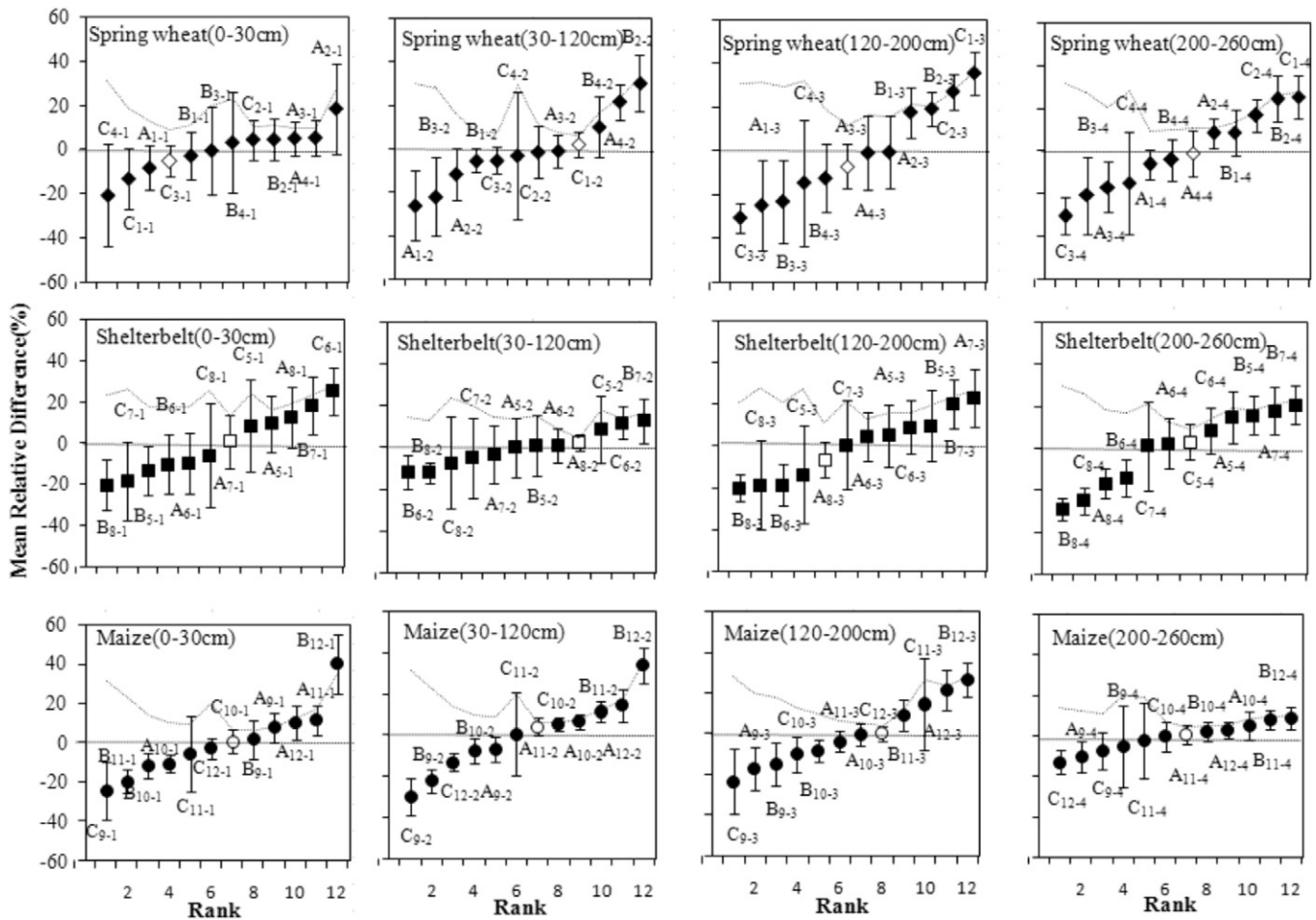


Fig. 7. Ranked mean relative differences (MRD) of soil water contents of four soil layers under three land use types indicated by the three types of symbols. Error bars represent the standard deviation of relative difference (SDRD). The most time-stable locations are indicated by the empty symbols. The curve indicates the index of time stability (ITS).

could be used to investigate the soil water relations between adjacent land use types.

The correlation coefficients relating SWC values between adjacent land use types at different distances from their common borders are presented in Table 5. The value of the SWC used for calculating the correlation coefficient at each distance was the mean value for three replications each of which was along a different transect. The soil water relation between adjacent subplots was affected by both the distance from the border and the depth of the soil layer. In the deepest layer (200–260 cm), all locations had a significant soil water relation among

themselves ($p < 0.01$). In contrast, significant soil water relations only occurred among close locations between adjacent land use types in the 120–200 cm soil layer. In the 30–120 cm soil layer, there were no significant correlations between the SWCs at any distance for the locations under the shelterbelt and maize subplots, but some significant correlations occurred between close locations under the spring wheat and shelterbelt subplots.

4. Discussion

4.1. Soil water content variations under different land use types

Soil water contents in the different soil layers under each land use type differed significantly and followed the same descending order: 200–260 > 120–200 > 0–120 cm (Fig. 4). This pattern was mainly attributed to the different effects of groundwater recharge, evaporation, and root water uptake. The 200–260 cm soil layer could be sufficiently recharged by the groundwater due to the shallowness of the water table, which ranged from a depth of 220 to 321 cm (Fig. 3). The top soil layer (0–120 cm) dried rapidly because of the high evaporation rate in this arid area (Chang et al., 2006; Zhao and Liu, 2010) and the large amounts of root water uptake by spring wheat, maize, and trees in order to meet their high transpiration demands (Shen et al., 2014; White and Kirkegaard, 2010). Soil water contents in the 0–120 cm layer exhibited different trends among the three land use types. In the spring wheat subplot, SWCs were similar in the 0–30 and 30–120 cm soil layers because soil water originating from both irrigation and rainfall were consumed by the crop roots, 87% of which were concentrated

Table 3

Statistical summary of the standard deviation of relative difference (SDRD) for soil water content in four soil layers under each of the three land use types.

SDRD(%)	0–30 cm	30–120 cm	120–200 cm	200–260 cm
Maximum				
Spring wheat	23.29	29.11	28.99	23.57
Trees	25.20	22.11	23.69	20.89
Maize	19.01	20.11	22.71	20.28
Minimum				
Spring wheat	7.00	5.45	6.99	6.89
Trees	11.54	4.15	6.37	5.34
Maize	4.56	3.24	3.88	3.88
Mean				
Spring wheat	13.54ab	12.30a	14.33a	11.21a
Trees	15.58a	11.97ab	14.58a	10.14a
Maize	9.20b	7.06b	9.53a	8.28a

Mean values followed by the same letter indicate that there was no significant difference ($p < 0.01$) between the SDRD of a given soil layer under two different land uses.

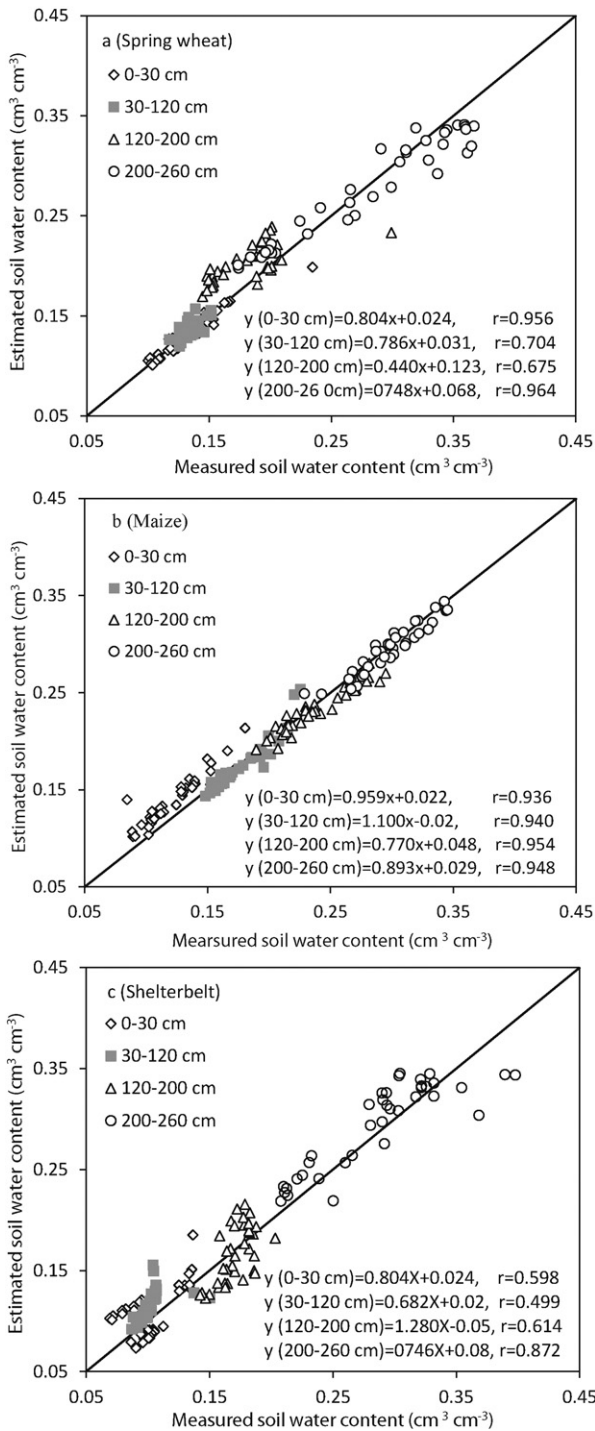


Fig. 8. Comparisons of measured soil water contents at the most time-stable location (MTSL) with the estimated values in the four soil layers under the three land use types. The solid line is the 1:1 line.

in the 0–120 cm soil layer (White and Kirkegaard, 2010). In contrast, under maize, SWCs were significantly greater ($p < 0.01$) in the 30–120 cm soil layer than in the 0–30 cm soil layer. This was because 90% of the maize roots were concentrated in the 0–30 cm soil layer and depleted the soil water from this layer (Shen et al., 2014). At the same time, excess irrigation water could percolate into the lower layer where it was unavailable to the crop thereby increasing the SWC. The SWC values in the 200–260 cm soil layer were always larger than those in the other soil layers (Fig. 4a and b). This percolation was found to account for 43% of the irrigation water applied to the maize

field (Ji et al., 2007). Therefore, the upper soil water profile was influenced by irrigation events differently under the two crops. In the non-irrigated shelterbelt subplot, SWCs were only greater in the 0–30 cm than in the 30–120 cm layer following certain rainfall events (Fig. 4c).

All of the correlations between SWCs in adjacent soil layers were significant ($p < 0.01$) while those between non-adjacent soil layers were not significant (Table 2). This was because the layers were affected by different factors. The two upper soil layers were mainly affected by rainfall and irrigation events, while the two lower layers were primarily influenced by groundwater recharge. In addition the correlations were stronger among the three upper layers ($r: 0.74$ to 0.89) than between the lowest layer and any other layer ($r: 0.39$ to 0.63). This reflected the similarity in SWCs in the upper three layers that varied similarly and were attributed to the increased percolation of irrigation water, which was then retained by the middle layers of the soil profile, due to the shallow roots of maize that were concentrated in the upper layer (Shen et al., 2014). In the shelterbelt subplot, SWCs were relatively weakly related in the top two soil layers ($r = 0.51$) while stronger relations existed between the two middle layers ($r = 0.87$) and between the two lower layers ($r = 0.74$). The weaker correlation between SWCs in the top two layers was due to rainfall events, which resulted in greater increases and greater variability in the SWCs in the upper layer than in the layer below it.

The soil water profiles in the upper 0–200 cm layer differed significantly among the three land use types ($p < 0.01$) (Fig. 5). The main reason was due to the occurrence and number of irrigation events as well as the amount of irrigation water applied. During the study period, irrigation was applied on 24 and 21 events to the maize and spring wheat subplots, respectively, while no direct irrigation of the shelterbelt subplot occurred. In addition, irrigation was applied at different times to the two crops in order to meet their respective requirements.

Rainfall interception by the canopy was also a factor resulting in differences in the SWCs of the 0–200 cm layer. Due to their relatively low degree of cover and the relatively short time in which they provided cover, the two crops did not intercept as much rainfall as the closed canopy of the Gansu Poplars. The tree canopy could reduce the amount of rainwater that infiltrated the soil by 14%–28% (Wallace et al., 1995); rainwater intercepted by the tree canopy was susceptible to evaporation and little stemflow reached the soil surface (Young, 1997). The overall effect was to generate SWCs in the 0–200 cm soil layer that were the highest under maize, while those under spring wheat were higher than those under the trees. The soil water distributions in the 0–200 cm layer contrasted with those in the 200–260 cm layer. The SWCs were notably greater in the lower-layer than in the upper-layer (Fig. 5) and there were no significant differences among the land use types ($p < 0.01$). This was mainly attributed to groundwater recharge. Groundwater uptake by vegetation was vital for the sustainable growth of the shelterbelt in this arid inland river basin. Miller et al. (2010) reported that groundwater recharge accounted for 80% of the evapotranspiration by *Quercus douglasii* during the dry summer in a semiarid oak savannah where the water table depth was between 700 and 1200 cm.

4.2. Spatial and temporal stability of soil water under different land use types

In this study, the spatial variability of SWCs in the field could be described by the range of the MRD. The MRD among the 0–30, 30–120 and 120–200 cm soil layers had similar ranges (Fig. 9a), and this indicates that the spatial variability of SWC in the three soil layers was also similar. The 200–260 cm soil layer had a relatively lower range of MRD as a result of the groundwater recharge. The MRD ranged within the values of -30% to $+30\%$ (Fig. 7) for the three land use types demonstrating moderate spatial variability. In our study area, the soil was relatively homogeneous over uniform topography. The MRD range in our study was comparable to that reported by Martinez et al. (2013) for a study site with homogeneous soil textures, where the ranges of soil water MRD

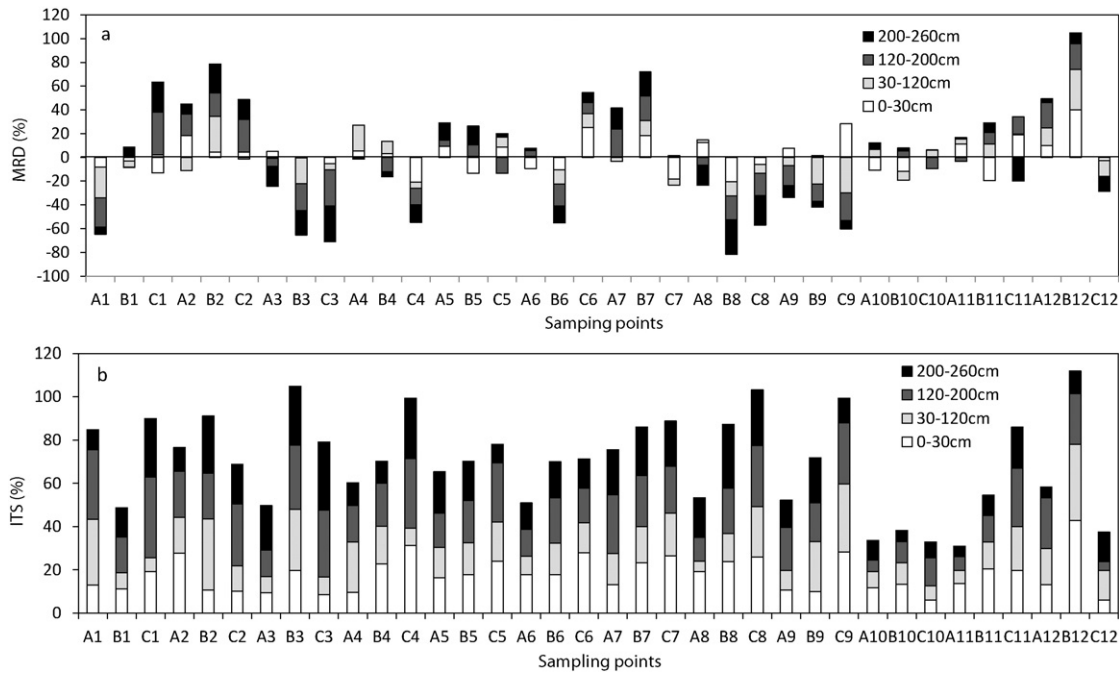


Fig. 9. Histogram of cumulated mean relative difference (MRD, a) and index of temporal stability (ITS, b) for each sampling point in the four soil layers.

were within -25% to $+25\%$. Similar results of the same order of magnitude were published by other researchers (Coppola et al., 2011; Liu and Shao, 2014; Martínez-Fernández and Ceballos, 2003). The ranges of MRD would be larger with increasing heterogeneity of factors that affected the spatial variability of SWC. Brocca et al. (2009) and Schneider et al. (2008) reported that the range of MRD for SWC increased with larger sampling scales due to an associated expected increase in the variability in soil textures, topography, vegetation types, etc. The ITS values in the 30–120 cm soil layer were lower than that in the upper soil layer (0–30 cm) because this soil layer was less affected by rainfall and evapotranspiration (Fig. 9b). The ITS values in the 200–260 cm soil layer were high and varied little due to the similar groundwater recharge under the three land use types. The maize subplot had the lowest value ITS among the three land use types because 90% of the maize roots were mainly concentrated in the 0–30 cm soil layer (Shen et al., 2014).

Temporal stability of SWC was characterized by the SDRD of the SWCs. The maize subplot had the highest temporal stability of SWC throughout the profile (Table 3). This result was mainly due to the relatively homogeneous effects caused by irrigation in combination with the effects of the shallow roots of the maize. The roots of the maize were mainly concentrated in the 0–30 cm layer. Consequently, irrigation was controlled to maintain a relatively steady SWC in this upper layer. Excess irrigation water drained and increased the SWCs at depths below 30 cm, which were not subject to maize root water uptake but were affected by drainage processes that occurred at a relatively steady rate. Thus, while fluctuations occurred between irrigation events, a relatively stable temporal system developed in the 0–200 cm soil layer. It

Table 4

Correlation coefficients for comparisons between two land use types of the measured soil water contents at the most temporally stable locations (MTSL) of the four soil layers.

Soil layer (cm)	Pearson correlation coefficient		
	Spring wheat and shelterbelt	Maize and shelterbelt	Maize and spring wheat
0–30	0.35**	0.44**	0.23
30–120	0.14	0.12	0.08
120–200	0.80**	0.39**	0.21
200–260	0.93**	0.82**	0.78**

** Significance level less than 0.01.

should also be noted that the practice of excessive irrigation in order to leach salts from the soil profile in the cropland was a factor in producing the stable temporal system. In the layer below 200 cm, the effects of the fluctuations in the water table induced a greater degree of SWC temporal stability (Table 3). In the 200–260 cm layer, the groundwater recharge, which was temporally stable, was the dominating factor affecting SWC whereas the effect of root water uptake was a minor factor. The SWCs in the 120–200 and 200–260 cm soil layers had similar degrees of temporal stability among the three land uses based on the SDRD values ($p < 0.01$), while in the 0–30 and 30–120 cm soil layers there were differences among the land uses (Table 3).

Measurements of SWC made at the MTSLs were found to reasonably estimate the mean SWC values of the various soil layers under each land use type. A number of studies have successfully used such measurements at the MTSLs to estimate the spatial mean SWC or soil water storage at different depths (Brocca et al., 2009; Zhao et al., 2010; Liu and Shao, 2014; Penna et al., 2013; She et al., 2015). Our results indicated that, at least in this study of the three land use types, a single location under each land use could be used to estimate the mean SWCs of each of the various layers under that land use type over multiple years. It should be noted that the MTSLs in our study could change if the crop and/or the irrigation regime was changed.

4.3. Soil water relations between adjacent land use types

The soil water relations between the cropland and shelterbelt play an important role in the survival of trees facing potentially severe drought conditions in arid and semiarid areas. The roots of the trees in the shelterbelt were able to uptake water from the deepest soil layer investigated in this study, where the SWC was typically maintained at higher levels than in the shallower layers due to the groundwater recharge. However, soil water from areas adjacent to the shelterbelt was also an important water source for the trees that could be taken up by roots that extended into the cropland areas (Cubera and Moreno, 2007; Shen et al., 2014). Shen et al. (2014) reported that Gansu Poplar roots could extend into maize cropland for a distance of at least 18 m. Karray et al. (2008) quantitatively estimated that olive root water uptake from cropland under irrigation contributed 50% of the water required for transpiration by adjacent olive trees in Central Tunisia.

Table 5

Correlation coefficient matrix of soil water contents of the four soil layers at different distances from the border between adjacent land use types.

	Distance from the border (m)	Location in spring wheat subplot				Distance from the border (m)	Location in maize subplot			
		1.0	6.67	12.34	18.01		1.0	6.67	12.34	18.01
0–30 cm layer										
Location in shelterbelt	3.5	0.08	0.29	0.32**	0.38**	2.5	0.34**	0.35**	0.29	0.31**
	13.5	−0.08	−0.03	0.06	0.05	12.5	0.36**	0.32	0.32	0.38**
	23.5	0.08	0.40**	0.42**	0.45**	22.5	0.18	0.15	0.13	0.11
	33.5	0.01	0.18	0.24	0.31	32.5	0.22	0.23	0.18	0.21
30–120 cm layer										
Location in shelterbelt	3.5	0.59**	−0.15	−0.30	−0.34**	2.5	0.30	0.27	0.27	0.29
	13.5	0.39**	0.33**	0.22	0.11	12.5	0.25	0.15	0.24	0.22
	23.5	0.44**	0.25	0.33**	0.21	22.5	0.08	0.00	0.09	0.06
	33.5	0.13	0.02	−0.04	0.04	32.5	0.08	−0.01	−0.07	−0.08
120–200 cm layer										
Location in shelterbelt	3.5	0.93**	0.48**	−0.24	−0.04	2.5	0.49**	0.29	0.18	0.29
	13.5	0.45**	0.70**	0.38**	0.22	12.5	0.43**	0.57**	0.49**	0.38**
	23.5	0.24	0.65**	0.60**	0.06	22.5	0.49**	0.48**	0.40**	0.30
	33.5	0.18	−0.17	−0.17	0.48**	32.5	0.23	0.10	0.03	0.04
200–260 cm layer										
Location in shelterbelt	3.5	0.94**	0.87**	0.88**	0.83**	2.5	0.83**	0.84**	0.76**	0.83**
	13.5	0.92**	0.92**	0.93**	0.88**	12.5	0.79**	0.85**	0.78**	0.79**
	23.5	0.83**	0.90**	0.91**	0.86**	22.5	0.77**	0.74**	0.70**	0.73**
	33.5	0.82**	0.89**	0.88**	0.87**	32.5	0.77**	0.77**	0.67**	0.65**

** Significance level less than 0.01.

Soil water in the 0–160 cm layer exhibited a decreasing trend with increasing proximity to the shelterbelt under both spring wheat and maize (Fig. 5). Similar trends have been reported for hedge–maize (Rosecrance et al., 1992) and grevillea–maize systems (Livesley et al., 2004). These SWC gradients were the result of the water uptake by the extended root systems of the trees or shrubs separating the crops (Shen et al., 2014). These gradients are reflected in the distributions of the fine tree roots in the crop subplots, where the root biomass decreased logarithmically with the increasing distance from the borders between the crops and the trees (Shen et al., 2014). Moreover, the correlation coefficients were only significant for the SWC between locations closer to the borders (Table 5).

The soil water relations between adjacent plots in the deepest soil layer under the three land use types were determined mainly by the groundwater recharge. Similar levels of groundwater recharge occurred in this layer under all three land uses and, thus, the SWCs among them were highly correlated. The water table under the three land uses was maintained at a high level due to the addition of percolating excess irrigation water from the cropland areas. Furthermore, the water table level rose during the irrigation season. Therefore, both the deep percolation of irrigation water in the deepest soil layer and the soil water in the upper soil layers under the crops that was accessible to tree root uptake were both important water sources that sustained the growing shelterbelts. Consequently, SWC under the crops depended on the soil depth and the distances from the borders between the plots due to the uptake of soil water by the tree roots.

5. Conclusions

In this study, the soil water dynamics were measured in the 0–260 cm layer during 2012 and 2013 along three transects passing through a spring wheat–shelterbelt–maize plot in an oasis region. The soil water relations between adjacent land use types were analyzed using the measured SWC at the identified MTSLs. The following conclusions could be drawn from this study:

- (1) Soil water contents in different soil layers were significantly different ($p < 0.01$) and decreased in the order: 200–260 cm > 120–200 cm > 0–120 cm under each land use type. In the same soil layer among the three land use types, temporal variations in soil water tended to have similar patterns.

- (2) The temporal stability of SWC in the 0–30 and 30–120 cm soil layers was significantly affected ($p < 0.01$) by the three different land use types. The temporal stability of SWC in the different soil layers was greater under maize than under either spring wheat or trees. The MTSLs were found for each soil layer under each land use type, and it was established that the measured SWC in a particular soil layer at the MTSLs could be used to estimate the mean SWCs for each of the subplots for the different soil layers.
- (3) The SWC measured at the MTSLs in the different soil layers under each land use type could be used to analyze soil water interactions between adjacent land use types. The three land use type subplots only affected adjacent subplots. In the 0–200 cm soil layer, soil water relations frequently occurred between locations close to the borders due to water uptake by tree roots that extended laterally into this soil layer under the cropland. The soil water relations in the lower soil layer (200–260 cm) among spring wheat, shelterbelt, and maize subplots were mainly due to groundwater recharge.

Acknowledgements

This research was financially supported by the National Natural Science Foundation of China (NSFC-RCUK_NERC, No. 41571130082). We would like to thank the Linze Inland River Basin Comprehensive Research Station, Chinese Ecosystem Research Network.

References

- Beguéría, S., Spanu, V., Navas, A., Machín, J., Angulo-Martínez, M., 2013. Modeling the spatial distribution of soil properties by generalized least squares regression: toward a general theory of spatial variates. *J. Soil Water Conserv.* 68 (3), 172–184.
- Brocca, L., Melone, F., Moramarco, T., Morbidelli, R., 2009. Soil moisture temporal stability over experimental areas in Central Italy. *Geoderma* 148 (3), 364–374.
- Chang, X., Zhao, W., Zhang, Z., Su, Y., 2006. Sap flow and tree conductance of shelter-belt in arid region of China. *Agric. For. Meteorol.* 138 (1), 132–141.
- Coppola, A., Comegna, A., Dragonetti, G., Lamaddalena, N., Kader, A., Comegna, V., 2011. Average moisture saturation effects on temporal stability of soil water spatial distribution at field scale. *Soil Tillage Res.* 114 (2), 155–164.
- Cubera, E., Moreno, G., 2007. Effect of land-use on soil water dynamic in dehesas of Central–Western Spain. *Catena* 71 (2), 298–308.

- Ellis, T., Hatton, T., Nuberg, I., 2005. An ecological optimality approach for predicting deep drainage from tree belts of alley farms in water-limited environments. *Agric. Water Manag.* 75 (2), 92–116.
- Grayson, R.B., Western, A.W., 1998. Towards areal estimation of soil water content from point measurements: time and space stability of mean response. *J. Hydrol.* 207 (1), 68–82.
- Hu, W., Shao, M., Wang, Q., Reichardt, K., 2009. Time stability of soil water storage measured by neutron probe and the effects of calibration procedures in a small watershed. *Catena* 79 (1), 72–82.
- Hu, W., Shao, M., Han, F., Reichardt, K., Tan, J., 2010. Watershed scale temporal stability of soil water content. *Geoderma* 158 (3), 181–198.
- Hu, W., Schoenau, J.J., Si, B.C., 2015. Representative sampling size for strip sampling and number of required samples for random sampling for soil nutrients in direct seeded fields. *Precis. Agric.* 16, 385–404.
- Hurlbert, S.H., 1984. Pseudoreplication and the design of ecological field experiments. *Ecol. Monogr.* 54 (2), 187–211.
- Huxley, P., Pinney, A., Akunda, E., Muraya, P., 1994. A tree/crop interface orientation experiment with a *Grevillea robusta* hedgerow and maize. *Agrofor. Syst.* 26 (1), 23–45.
- Ji, X., Kang, E., Chen, R., Zhao, W., Zhang, Z., Jin, B., 2007. A mathematical model for simulating water balances in cropped sandy soil with conventional flood irrigation applied. *Agric. Water Manag.* 87 (3), 337–346.
- Kachanoski, R., Jong, E., 1988. Scale dependence and the temporal persistence of spatial patterns of soil water storage. *Water Resour. Res.* 24 (1), 85–91.
- Karray, J.A., Lhomme, J.-P., Masmoudi, M., Mechlia, N.B., 2008. Water balance of the olive tree–annual crop association: a modeling approach. *Agric. Water Manag.* 95 (5), 575–586.
- Knight, A., Blott, K., Portelli, M., Hignett, C., 2002. Use of tree and shrub belts to control leakage in three dryland cropping environments. *Crop Pasture Sci.* 53 (5), 571–586.
- Lark, R.M., Cullis, B.R., 2004. Model-based analysis using REML for inference from systematically sampled data on soil. *Eur. J. Soil Sci.* 55, 799–813.
- Li, X., He, M., Jia, R., 2008. The response of desert plant species diversity to the changes in soil water content in the middle-lower reaches of the heihe river. *Adv. Earth Sci.* 7, 012.
- Liu, B., Shao, M., 2014. Estimation of soil water storage using temporal stability in four land uses over 10 years on the loess plateau, China. *J. Hydrol.* 517, 974–984.
- Livesley, S.J., Gregory, P., Buresh, R., 2004. Competition in tree row agroforestry systems. 3. soil water distribution and dynamics. *Plant Soil* 264 (1–2), 129–139.
- Luo, F., Qi, S., Xiao, H., 2005. Landscape change and sandy desertification in arid areas: a case study in the zhangye region of Gansu province, China. *Environ. Geol.* 49 (1), 90–97.
- Malik, R., Sharma, S., 1990. Moisture extraction and crop yield as a function of distance from a row of *Eucalyptus tereticornis*. *Agrofor. Syst.* 12 (2), 187–195.
- Martinez, G., Pachepsky, Y.A., Vereecken, H., Hardelauf, H., Herbst, M., Vanderlinden, K., 2013. Modeling local control effects on the temporal stability of soil water content. *J. Hydrol.* 481, 106–118.
- Martínez-Fernández, J., Ceballos, A., 2003. Temporal stability of soil moisture in a large-field experiment in Spain. *Soil Sci. Soc. Am. J.* 67 (6), 1647–1656.
- Martínez-Fernández, J., Ceballos, A., 2005. Mean soil moisture estimation using temporal stability analysis. *J. Hydrol.* 312 (1), 28–38.
- Miller, G.R., Chen, X., Rubin, Y., Ma, S., Baldocchi, D.D., 2010. Groundwater uptake by woody vegetation in a semiarid oak savanna. *Water Resour. Res.* 46 (10), W10503. <http://dx.doi.org/10.1029/2009WR008902>.
- Nair, P.K.R., 1985. *Agroforestry in the Context of Land Clearing and Development in the Tropics*. International Council for Research in Agroforestry.
- Nair, P.K.R., 1993. *An Introduction to Agroforestry*. Kluwer Academic Publishers, Dordrecht, The Netherlands.
- Nestel, B., 1983. *Agricultural Research for Development: Potentials and Challenges in Asia*. Agricultural Research for Development: Potentials and Challenges in Asia, Jakarta (Indonesia), 24–29 Oct 1982. ISNAR.
- Ong, C., Odongo, J., Marshall, F., Black, C., 1992. *Water Use of Agroforestry Systems in Semi-Arid India*. John Wiley and Sons, Inc., New York, NY (United States).
- Penna, D., Brocca, L., Borga, M., Dalla Fontana, G., 2013. Soil moisture temporal stability at different depths on two alpine hillslopes during wet and dry periods. *J. Hydrol.* 477, 55–71.
- Rosecrance, R.C., Brewbaker, J., Fownes, J., 1992. Alley cropping of maize with nine leguminous trees. *Agrofor. Syst.* 17 (2), 159–168.
- SAS Institute Inc., 2008. *SAS/STAT users' guide*. Release 9.2 ed. SAS Institute Inc., Cary, NC.
- Schneider, K., Huisman, J., Breuer, L., Zhao, Y., Frede, H.-G., 2008. Temporal stability of soil moisture in various semi-arid steppe ecosystems and its application in remote sensing. *J. Hydrol.* 359 (1), 16–29.
- She, D., Zhang, W., Hopmans, J.W., Carlos, T.L., 2015. Area representative soil water content estimations from limited measurements at time-stable locations or depths. *J. Hydrol.* 530, 580–590.
- Shen, Q., Gao, G., Fu, B., Lü, Y., 2014. Soil water content variations and hydrological relations of the cropland-treebelt-desert land use pattern in an oasis-desert ecotone of the Heihe River basin, China. *Catena* 123, 52–61.
- Vachaud, G., Passerat de Silans, A., Balabanis, P., Vauclin, M., 1985. Temporal stability of spatially measured soil water probability density function. *Soil Sci. Soc. Am. J.* 49 (4), 822–828.
- Vanderlinden, K., et al., 2012. Temporal stability of soil water contents: a review of data and analyses. *Vadose Zone J.* 11 (4). <http://dx.doi.org/10.2136/vzj2011.0178>.
- Wallace, J., Jackson, N., Ong, C., 1995. *Water balance of agroforestry systems on hillslopes*. Final Report to the ODA Forestry Research Programme.
- Wang, G., Liu, J., Kubota, J., Chen, L., 2007. Effects of land-use changes on hydrological processes in the middle basin of the Heihe River, Northwest China. *Hydrol. Process.* 21 (10), 1370–1382.
- White, R.G., Kirkegaard, J.A., 2010. The distribution and abundance of wheat roots in a dense, structured subsoil—implications for water uptake. *Plant Cell Environ.* 33 (2), 133–148.
- Williams, C., McNamara, J., Chandler, D., 2009. Controls on the temporal and spatial variability of soil moisture in a mountainous landscape: the signature of snow and complex terrain. *Hydrol. Earth Syst. Sci.* 13 (7), 1325–1336.
- Woodall, G., Ward, B., 2002. Soil water relations, crop production and root pruning of a belt of trees. *Agric. Water Manag.* 53 (1), 153–169.
- Young, J., 1997. *Agroforestry for Soil Management*. CAB/ICRAF, Wallingford, UK.
- Zhao, W., Liu, B., 2010. The response of sap flow in shrubs to rainfall pulses in the desert region of China. *Agric. For. Meteorol.* 150 (9), 1297–1306.
- Zhao, Y., Peth, S., Wang, X., Lin, H., Horn, R., 2010. Controls of surface soil moisture spatial patterns and their temporal stability in a semi-arid steppe. *Hydrol. Process.* 24 (18), 2507–2519.